Title	Hydrogen bonding in crystal forms of primary amide functionalized glucose and cellobiose
Authors	Moynihan, Humphrey A.;Hayes, John A.;Eccles, Kevin S.;Coles, Simon J.;Lawrence, Simon E.
Publication date	2013-06
Original Citation	MOYNIHAN, H. A., HAYES, J. A., ECCLES, K. S., COLES, S. J. & LAWRENCE, S. E. 2013. Hydrogen bonding in crystal forms of primary amide functionalised glucose and cellobiose. Carbohydrate Research, 374, 29-39. http://dx.doi.org/10.1016/j.carres.2013.03.024
Type of publication	Article (peer-reviewed)
Link to publisher's version	http://www.sciencedirect.com/science/article/pii/S0008621513001122 - 10.1016/j.carres.2013.03.024
Rights	© 2013 Elsevier Ltd. All rights reserved. NOTICE: this is the author's version of a work that was accepted for publication in Carbohydrate Research. Changes resulting from the publishing process, such as peer review, editing, corrections, structural formatting, and other quality control mechanisms may not be reflected in this document. Changes may have been made to this work since it was submitted for publication. A definitive version was subsequently published in Carbohydrate Research, [Volume 374, 7 June 2013, Pages 29–39] DOI http://dx.doi.org/10.1016/j.carres.2013.03.024 - https://creativecommons.org/licenses/by-nc-nd/4.0/
Download date	2025-05-14 04:25:27
Item downloaded from	https://hdl.handle.net/10468/1588

University College Cork, Ireland
Coláiste na hOllscoile Corcaigh

Hydrogen bonding in crystal forms of primary amide functionalized glucose and cellobiose

Humphrey A. Moynihan[a*], John A. Hayes[a], Kevin S. Eccles[a], Simon J. Coles[b], Simon E. Lawrence[a]

[a]*Department of Chemistry / Analytical and Biological Chemistry Research Facility, University College Cork, College Road, Cork, Ireland*

[b]*UK National Crystallographic Service, School of Chemistry, University of Southampton, Highfield, Southampton, SO17 1BJ, UK*

ABSTRACT

A glucoside and cellobioside of glycolamide were synthesised and the crystal chemistry of these compounds investigated. The amidoglucoside crystallised in the $P2_1$ space group. The primary amide group participates in C(7) and C(17) chains also involving the pyranose oxygen and hydroxyl groups. The amidocellobioside crystallised as a methanol solvate in the $P2_1$ space group. The amide N-H groups donate hydrogen bonds to oxygen atoms on the cellobiose units, while intramolecular hydrogen bonds give rise to S(7) and S(9) motifs in addition to a $R_3^3(9)$ motif. A tetra-*O*-acetylglucoside derivative of thioglycolamide and its

[*] Corresponding author. Tel: +353 21 4902488; Fax: +353 21 4274097

E-mail address: h.moynihan@ucc.ie

sulfoxide derivative were synthesied to examine the effect of protecting the glucopyanose hydroxyl groups. The thioglycolamido derivative, which crystallised in the $P2_12_12_1$ space group, featured amide N-H groups donating to the glucopyranose oxygen and an acetyloxy group. The sulfoxy derivative crystallised in the $P2_1$ space group and featured the primary amide groups forming $R_3^2(8)$ motifs generating a $P2_1$ ladder.

Keywords: Glucose, Cellobiose, Primary amides, Crystal engineering

1. Introduction

Crystal engineering is the control of molecular assembly in crystals with the ultimate aim of controlling properties which arise from the collective participation of molecules in the crystalline array such as density, melting point, solubility, mechanical and thermal characteristics.[1] For sugars and carbohydrates, these crystal state properties affect activities such as hygroscopicity, flow, blending, compression into tablets and other operations of commercial importance.[2] An ability to control the molecular assembly of sugar molecules in crystalline solids in a rational manner would have applications in areas such as pharmaceutical formulation using sugar-derived excipients. Crystal engineering exploits 'supramolecular synthons', these being structural units within crystals which assemble by known intermolecular interactions.[3] Amides, which form well known hydrogen bonded

motifs in the solid state, are good examples of such synthons.[4] In particular, primary amide groups are associated with important supramolecular motifs often occurring in crystal structures, such as dimers and 'amide ladders'.[5] These motifs are conveniently described using the notation devised by Etter, for example the common amide dimer motif can be described as an $R_2^2(8)$ dimer.[6] The functional groups generally present in sugars: alcohols, acetals and ketals, have not been widely exploited in crystal engineering. The crystal chemistry of sugars generally focuses on features such as pyranose ring puckering characterised by Cremer-Pople parameters,[7] torsional angles for primary hydroxyls and acetal linkages[8] and conformational or supramolecular features specific to classes of monosaccharide or polysaccharide.[9]

Carefully designed structural modifications can be used to provide insights into physical or crystallographic aspects of sugars. For example, modified sugars can provide information of the details of enzyme-sugar binding,[10] can act as models for complex biomolecules[11] or can provide information on interactions between sugar-based groups.[12] The work described herein aims to investigate whether incorporation of conventional supramolecular synthons, in particular primary amides, into sugars gives rise to motifs such as $R_2^2(8)$ dimers, which could be used as a basis for crystal engineering; or whether alternatively, the hydrogen bonding capabilities of the sugar and amide group form new exploitable motifs. To achieve this aim, a short series of primary amido-functionalised glucose and cellobiose derivatives have been prepared and the crystal chemistry of these determined. These molecules are designed to have distinct sugar and amide domains in contrast to, for example, *N*-acetylglucosamine, in which the amide group is directly substituted on the glucopyranose ring. Crystallisation and crystal structure determination of the resulting primary amide

functionalised glucose and cellobiose compounds were then carried out to probe the hydrogen bonding networks thus formed.

2. Results and discussion

2.1. Preparation of primary amide functionalised glucose and cellobiose derivatives

Primary amide functionalized derivatives of glucose and cellobiose were synthesized from the corresponding trichloroacetimidates as outline in Scheme 1, *i.e* by conversion of the trichloroacetimdates **1** and **5** to the corresponding methyl glycolate derivates **2** and **6**, followed by treatement of these with ammonia in methanol to give the required primary amide functionalised glucose and cellobiose derivatives, **3** and **7** respectively.

<Scheme 1 about here>

2.2. Crystal structures of primary amide functionalised glucose 3 and cellobiose 7

Crystals of compounds **3** and **7** suitable for analysis by single-crystal X-ray diffraction were grown by slow evaporation of solutions in ethanol and methanol respectively. Both compounds crystallized in the monoclinic $P2_1$ space group. Crystallographic data are given in Table 1. Table 2 gives the hydrogen bond data obtained from PLATON.[13]

<Table 1 about here>

<Table 2 about here>

The glucopyranose ring of compound **3** adopts a $^4C_1$ conformation with the corresponding Cremer-Pople parameters given in Table 3. These values are close to the corresponding values for an ideal cyclohexane chair (Q = 0.63 Å, θ = 5.0 °).[7] The dihedral angle around the primary hydroxyl group on C-6 is 75.54 ^{o} indicating a *gauche-trans* conformation. The primary amide forms a discrete hydrogen bond between one of the amide N-H and the heterocyclic oxygen of an adjacent glucopyranose ring, forming C(7) chains along the *b* axis (Figure 1 and 2), i.e. hydrogen bonded chains consisting of a repeat unit containing 7 atoms. The amide oxygen also accepts a hydrogen bond from the primary hydroxyl, forming a C(17) chain with two molecules in the repeat unit (Figures 3 and 4). It should be noted that while crystallisation from ethanol gave crystals (m.p. 155.0 °C by DSC) of compound **3** suitable for single-crystal XRD, crystallisation from methanol gave crystals of melting point 165.5 °C (DSC), possibly another crystal form such as a polymorph or solvate. However these latter crystals were highly agglomerated and were not suitable for single-crystal analysis.

<Table 3 about here>

<Figure 1 about here>

<Figure 2 about here>

<Figure 3 about here>

<Figure 4 about here>

Single-crystal XRD analysis of crystals of compound **7** shows that the form obtained was a methanol solvate. Cremer-Pople parameters (Table 3) for the glucopyranose rings of both the reducing end and the non-reducing end were consistent with $^4C_1$ conformations. The dihedral angle about the primary hydroxy group in the non-reducing pyranose is −60.75 ° while that for the reducing pyranose is −75.06 °, equivalent to *gauche-gauche* conformations in both cases. The angle at the oxygen joining the pyranose rings is 115.3 °. The amide N-H groups are donating hydrogen bonds to the 3-OH of one molecule and the 6'-OH of another, while the amide carbonyl accepts a hydrogen bond from the methanol molecule (Figure 5 and 6). Intramolecular hydrogen bonds are observed between O3-H and the oxygen of the non-reducing pyranose, and O2'-H and O6, giving rise to 7-membered and 9-membered intramolecular hydrogen bonded motifs, designated as S(7) and S(9) motifs respectively using Etter's notation (Figures 7 and 8).[6] A similar S(9) motif involving an O6-H...O2' bond was observed in the structure of cyclohexyl 4'-*O*-cyclohexyl β-D-cellobioside cyclohexane solvate.[14] The O2-H of a separate molecule accepts a hydrogen bond from the O6'-H and donates a hydrogen bond to the O3 forming a hydrogen bonded ring, designated as a R_3^3 (9) motif using Etter's notation,[6] which also involves the O3-H...O intramolecular hydrogen bond (Figure 7 and 8). In the structure, the molecules form layers that cross each other as shown in Figure 9, rather than a herringbone pattern. A comparable crystal structure for compound **7** is that of methyl β-cellobioside methanol solvate which also crystallised in the $P2_1$.[15] However, significant differences were observed in the interaction of the methanol molecule and in intramolecular hydrogen bonding. Whereas in compound **7**, the solvated methanol is

seen to hydrogen bond to the amide carbonyl, in the structure of methyl β-cellobioside methanol solvate the methanol molecule is hydrogen bonded to the primary hydroxyl of the reducing glucopyranose. Also in the structure of methyl β-cellobioside methanol solvate, the 3-position hydroxyl of the reducing glucopyranose is participating in a hydrogen bonded ring involving the non-reducing pyranose oxygen and primary hydroxyls, unlike the hydrogen bonding motifs illustrated in Figure 8.

Also in the structure of **7**.MeOH, there is a short contact of 2.1 Å between H1' and H4. Both C-H bonds are axial and approximately parallel. Compound **7** is a good subject for prediction of properties of a helix consisting of repetition of either of the glucopyranose rings. The parallel C1'-H and C4-H bonds would correspond to a twofold screw axis if present in an extended cellulose-like polymer.[16] Extrapolation of helix properties from crystal structure data of small molecule glucopyranose derivatives has been developed by French and Johnson as a technique for obtaining data on model cellulose chains.[17] The necessary input for the extrapolation are the virtual bond length of the glucopyranose residue, i.e. the O1-O4 distance, the virtual angle formed by two such rings and the virtual torsion angle formed by three such rings. Using the non-reducing glucopyranose of compound **7** as such a model and the formulae given by French and Johnson gives the predicted number of glucopyranose residues per turn of the model helix as −2.19, indicating a left-handed helix which advances 5.19 Å per glucopyranose residue. These values are within the ranges given by French and Johnson based on calculations using data from twenty-three small molecules.[17]

<Figure 5 about here>

<Figure 6 about here>

<Figure 7 about here>

<Figure 8 about here>

<Figure 9 about here>

2.3. Preparation of acetylated sulfide-amido, sulfoxide-amido and sulfonyl-amido glucose derivates

In the crystal structures for compounds **3** and **7** discussed above, the primary amide groups are involved in hydrogen bonding with pyranose hydroxyls or oxygens rather than generating familiar primary amide motifs such as 'amide ladders'. This is not very surprising as the glucopyranose groups offer extensive hydrogen bond donating and accepting capacity, although it might have been hoped that a degree of molecular recognition may have existed between the amide groups. This could be moderated by blocking the hydroxyls so as to reduce the hydrogen bond donating capacity of the glucopyranoses. Such derivatives would be protected glucosides and therefore would not display the full supramolecular characteristics of sugars in the crystalline solid state. However, informative supramolecular solid state chemistry would still be obtained and it would be possible to evaluate whether typical amide supramolecular motifs were possible with such systems under any circumstances. The sulfide and sulfoxide linked peracetylated glucosyl primary amides **9** and **10** were synthesized for this purpose. While the sulfide linkage in compound **9** was formed primarily to bind the amide and peracetyl glucose regions, the option of further oxidising these to the sulfoxide **10** and sulfone **11** was an obvious extension of the system (Scheme 2).

Amidosulfide **9** was obtained by reaction of glucose pentaacetate **8** with thiourea in the presence of $BF_3.Et_2O$, generating a thiouronoium intermediate *in situ* which was subsequently hydrolysed and the resulting thiolate reacted with chloroacetamide. Careful oxidation with Oxone® gave the sulfoxide **10**, while oxidation of **9** with *m*CPBA gave the sulfone **11**. Sulfoxide **10** appeared to be a single diastereoisomer by NMR although the yield of isolated product was very modest (33%) so that formation of some quantity of the epimeric sulfoxide which would have been removed during purification cannot be ruled out.

2.4. Crystal structures of acetylated sulfide-amido glucose derivative 9 **and sulfoxide-amido glucose derivate** 10

Crystals of compounds **9** and **10** suitable for single-crystal X-ray analysis were obtained by allowing undersaturated solutions of **9** and **10** in methanol to slowly evaporate at ambient temperature, however suitable crystals of sulfone **11** were not obtained. Crystallographic data for compounds **9** and **10** are given in Table 1.

<Scheme 2 about here>

Compound **9** crystallised in orthorhombic $P2_12_12_1$ space group. Cremer-Pople parameters (Table 3) are consistent with a $^4C_1$ conformation. The amide N-H groups donate hydrogen bonds to the pyranose oxygen and the carbonyl group of the 2-acetoxy group of adjacent molecules (Figures 10 and 11).

<Figure 10 about here>

<Figure 11 about here>

Compound **10** crystallised as monoclinic $P2_1$. Compound **10** has Cremer-Pople parameters (Table 3) relating to typical $^4C_1$ values. The primary amide groups form C(4) hydrogen bonded chains. In each amide group, the N-H not involved in the C(4) motif is donating a hydrogen bond to an amide carbonyl in a parallel chain forming a series of $R\,\frac{2}{3}\,(8)$ rings, giving rise to a ladder-like motif referred to as a 2_1 axis[18] (Figures 12 and 13), although not the more common 'amide ladder' composed of $R\,\frac{2}{2}\,(8)$ rings. The sulfur atom of the sulfoxide group is a stereogenic centre having *S* configuration. The packing observed in the structure of compound **10** would appear to maximize density as illustrated by Figure 14.

<Figure 12 about here>

<Figure 13 about here>

<Figure 14 about here>

2.5. Conclusion

Primary amide derivatives of glucose and cellobiose, compounds **3** and **7**, have been prepared and their crystal structures determined. These structures did not display common amide type motifs such as C(4) chains and $R\,\frac{2}{2}\,(8)$ dimers, but rather motifs involving both sugar and amide groups. For compound **3**, a C(17) chain with two molecules in the repeat unit was observed. For compound **7**, the amide N-H groups donated hydrogen bonds to oxygen atoms

on the cellobiose units, while intramolecular hydrogen bonds giving rise to S(7) and S(9) motifs were observed in addition to a $R_3^3(9)$ motif. Sulfide **9**, in which the glucopyranose hydroxyls were acetylated, displayed amide N-H groups donating to glucopyranose oxygen and an acetyloxy group. However, sulfoxide **10** displays an interesting ladder-like motif composed from $R_3^2(8)$ rings. This motif, also known as a primary amide 2_1 axis motif, is not as common as the amide ladder but has been observed in crystal structure of some primary amides, for example adipamide and 2-chlorobenzamide.[18]

The structures studied generally display individual hydrogen bonding patterns featuring motifs involving both primary amide and sugar groups rather than distinct amide-based and sugar-based motifs. In the case of the acetylated amidoglucosyl sulfoxide **10**, a characteristic primary amide motif was observed. Hence for three of the compounds studied, the degree of molecular recognition between the primary amide groups was not strong enough to drive formation of crystal structures based on distinct amide and sugar motifs, at least in the crystal forms obtained, while specific supramolecular interactions between the primary amide groups were observed in the acetylated sulfoxide **10**. This suggests that crystal engineering of sugars through exploitation of primary amide motifs may be possible. However, modification of the hydroxy groups and/or inclusion of further functionality may be necessary which would limit applications. Another possibility is that further research on the nucleation and growth of compounds such as **3** and **7** may generate new crystal forms with distinct amide and sugar motifs. Alternatively, modification of the amide functionality, e.g. addition or removal of methylene groups, may produce compounds with such crystal structures.

3. Experimental

3.1. General methods

All commercial reagents were purchased from Sigma-Aldrich and were used without further purification. All solvents were either of a HPLC grade or distilled prior to use. Column chromatography was conducted using Merck silica gel 60, typically with a 30:1 ratio of silica to sample. Infrared spectra were recorded on a Perkin-Elmer Paragon 1000 FT-IR spectrometer. The ^{1}H NMR spectra were recorded on a Bruker AVANCE 300 MHz spectrometer. Chemical shift values (δ_H and δ_C) are expressed as parts per million (ppm). Elemental analyses were performed by the Microanalysis Laboratory, University College Cork, using an Exeter Analytical CE440 elemental analyzer. High resolution mass spectra (HRMS) were recorded on a Waters LCT Premier LC-MS instrument in electrospray ionisation (ESI) positive mode using 50 % MeCN-H_2O containing 0.1 % HCO_2H as eluant; samples were made up in MeCN.

3.2. Synthesis

3.2.1. Methyl 1-*O*-(-2-Carboxy)methyl-2,3,4,6-tetra-*O*-acetyl-β-D-glucopyranose (2)

2,3,4,6-Tetra-*O*-acetyl-1-*O*-trichloroacetimidoyl-α-D-glucopyranose[19] **1** (1.50 g, 3.05 mmol) was stirred in dry CH_2Cl_2 (30 mL) along with methyl glycolate (0.26 mL, 3.36 mmol) over 4Å mol sieves at −25 ^{o}C. $BF_3.Et_2O$ (0.41 mL, 3.36 mmol) was added and the solution was allowed to slowly warm to room temperature. After 4 to 5 h, the solution was filtered and washed with sat. aq. $NaHCO_3$ soln. (2 × 20 mL), H_2O (2 × 20 mL) and brine (20 mL). The solvent was removed *in vacuo* and the resulting residue was purified with column chromatography using EtOAc: hexane to yield a white solid (0.95 g, 74%). IR (KBr); ν 2958 (C-H), 1756 (C=O), 1371 (CH), 1235 (O-C=O) and 1045 cm^{-1} (O-C-O); ^{1}H NMR ($CDCl_3$):

δ 1.95 (3H, s, OAc), 1.96 (3H, s, OAc), 2.02 (3H, s, OAc), 2.03 (3H, s, OAc), 3.63 (1H, ddd, ^{3}J = 9.0, 4.8, 2.4 Hz, H-5), 3.69 (3H, s, OCH_3), 4.07 (1H, dd, ^{2}J = 12.0, ^{3}J = 2.4 Hz, H-6), 4.19 (1H, dd, ^{2}J = 12.0, ^{3}J = 4.8 Hz, H-6'), 4.23 (2H, s, OCH_2CO_2Me), 4.60 (1H, d, ^{3}J = 7.8 Hz, H-1), 4.98 (1H, dd, ^{3}J = 9.0, 7.8 Hz, H-2), 5.02 (1H, t, ^{3}J = 9.0 Hz, H-4), 5.18 (1H, t, ^{3}J = 9.0 Hz, H-3); ^{13}C NMR ($CDCl_3$): δ 19.59 (CH_3), 19.60 (CH_3), 19.71 (CH_3), 19.72 (CH_3), 50.98 (OCH_3), 60.77 (*C*-6), 63.94 (CH_2), 67.29 (*C*-4), 69.92 (*C*-2), 70.93 (*C*-5), 71.50 (*C*-3), 99.11 (*C*-1), 168.42, 168.60, 168.66, 169.18, 169.65 (4 × O*Ac*, 1 × CO_2Me).

3.2.2. 1-*O*-(2-Carboxamido)methyl-β-D-glucopyranose (3)

Methyl 1-*O*-(-2-carboxy)methyl-2,3,4,6-tetra-*O*-acetyl-β-D-glucopyranose **2** (1.00 g, 2.39 mmol) was stirred in 2M NH_3 in MeOH soln. (20 mL, 40 mmol) for 1 h. The methanolic ammonia was removed under reduced pressure and the crude residue was recrystallised from a minimum of hot MeOH to yield a white solid (0.55 g, 99 %). Mp 165.49 ^{o}C; IR (KBr); ν 3422 (OH, NH), 2923 (CH), 1672 (NHC=O), 1379 (CH), 1325 (CH), 1222 (O-C=O) and 1132 cm^{-1} (C-O-C); ^{1}H NMR (d_6-DMSO): δ 3.41-3.48 (1H, m), 3.67 (1H, ddd, ^{3}J = 9.9, 6.3, 1.8 Hz), 3.89 (1H, d, ^{2}J = 15.0 Hz, OCH_2CO_2Me), 4.09 (1H, d, ^{2}J = 15.0 Hz, OCH_2CO_2Me), 4.16 (1H, d, ^{3}J = 9.0 Hz, H-1), 4.55 (1H, t, ^{3}J = 6.0 Hz), 4.95 (1H, d, ^{3}J = 6.0 Hz), 5.02 (1H, d, ^{3}J = 3.0 Hz), 5.51 (1H, d, ^{3}J = 3.0 Hz), 7.42 (2H, br s, NH_2); ^{13}C NMR (d_6-DMSO): δ 60.90 (CH_2), 47.81 (CH_2), 69.88 (CH), 73.35 (CH), 76.16 (CH), 76.98 (CH), 103.02 (*C*-1), 171.57 ($CONH_2$).

3.2.3. Preparation of α-D-Glucopyranose-4-*O*-(2,3,4,6-tetra-*O*-acetyl-β-D-glucopyranosyl)-2,3,6-triacetyl-1-*O*-trichloroacetimidate (5)

To a solution of β-D-glucopyranose-4-*O*-(2,3,4,6-tetra-*O*-acetyl-β-D-glucopyranosyl)-, 1,2,3,6-tetraacetate (**4**) (2.0 g, 2.94 mmol) in THF was added benzylamine[20] (0.35 mL, 3.24 mmol) and the solution was stirred at ambient temperature for 12 h. The solvent was removed *in vacuo* and the resulting syrup was dissolved in $CHCl_3$ (150 mL). The organic phase was washed with 1M HCl (2 × 30 mL), water (2 × 30 mL) and brine (30 mL), dried over $MgSO_4$ and the solvent removed under reduced pressure. The crude solid was subjected to column chromatography with ethyl acetate: hexane (1:1) as eluant, to yield α/β-D-glucopyranose-4-*O*-(2,3,4,6-tetra-*O*-acetyl-β-D-glucopyranosyl)-2,3,6-triacetate as a white solid (1.21 g, 64% yield) as a 3.2:1 mix of anomers (α:β) (by NMR integration) ^{1}H NMR ($CDCl_3$, α anomer) δ: 1.93 (3H, s), 1.96 (3H, s), 1.98 (3H, s), 2.02 (3H, s), 2.04 (3H, s), 2.08 (3H, s), 2.09 (3H, s), 3.64-3.61 (1H, m), 3.71 (1H, t, ^3J = 9.2 Hz), 3.82-3.96 (2H, m), 4.14 - 3.98 (1H, m), 4.30 (1H, dt, ^3J = 6.7, 3.9 Hz), 4.51 - 4.45 (2H, m), 4.79 - 4.69 (1H, m), 4.88 (1H, ddd, ^3J = 9.0, 6.0, 3.0 Hz), 5.16 - 4.99 (2H, m), 5.31 (1H, t, ^3J = 4.3 Hz), 5.45 (1H, t, ^3J = 9.0 Hz). ^{13}C NMR δ_C ($CDCl_3$): 20.64 (2xCH_3), 20.74 (2xCH_3), 20.85 (CH_3), 20.94 (2xCH_3), 61.77 (CH_2), 62.00 (CH_2), 68.00 (CH), 68.29 (CH), 69.55 (CH), 71.52 (CH), 71.83 (CH), 72.06 (CH), 72.22 (CH), 73.11 (CH), 73.19 (CH), 73.42 (CH), 90.15 (CH), 95.35 (C-1, unknown anomer), 100.96 (C-1, unknown anomer), 100.97 (CH), 169.30 (OAc), 169.56 (OAc), 169.96 (OAc), 170.53 (OAc), 170.64 (OAc), 170.84 (OAc), 170.92 (OAc). The α/β-D-glucopyranose-4-*O*-(2,3,4,6-tetra-*O*-acetyl-β-D-glucopyranosyl)-2,3,6-triacetate obtained (5.0 g, 7.86 mmol) and Cl_3CCN (1.57 mL, 15.72 mmol) were stirred in dry CH_2Cl_2 (80 mL) at 0 ^{o}C for 30 min. DBU (0.12 mL, 0.78 mmol) was added dropwise and the solution was allowed warm to room temperature and stirred for 12 h. The solvent was removed in *vacuo* and the residue was subjected to silica gel chromatography (40:60 EtOAc:hexane) to yield a foam (3.18 g, 52%); ^{1}H NMR ($CDCl_3$): δ 1.99 (3H, s, OAc), 2.01 (3H, s, OAc), 2.02 (3H,

OAc), 2.03 (3H, s, OAc), 2.04 (3H, s, OAc), 2.09 (3H, s, OAc), 2.10 (3H, s, OAc), 3.66 (1H, ddd, ^{3}J = 9.0, 6.0, 3.0 Hz, H-5'), 3.84 (1H, t, ^{3}J = 9.0 Hz, H-4), 4.02-4.15 (3H, m, H-5, H-6), 4.39 (1H, dd, ^{3}J = 12.0, 3.0 Hz, H-6'), 4.49-4.56 (2H, m), 4.94 (1H, t, ^{3}J = 9.0 Hz), 5.04-5.15 (3H, m, H-2), 5.53 (1H, t, ^{3}J = 9.0 Hz, H-3), 6.48 (1H, d, ^{3}J = 3.9 Hz, H-1), 8.66 (1H, s, NH); ^{13}C NMR ($CDCl_3$): δ 20.49 (*C*H_3), 20.57 (*C*H_3), 20.63 (2 × *C*H_3), 20.70 (2 × *C*H_3), 20.84 (*C*H_3), 61.38 (C-6), 61.55 (C-6'), 67.70 (*C*H), 69.29 (*C*H), 69.86 (*C*H), 70.96 (*C*H), 71.67 (*C*H), 72.02 (*C*H), 73.06 (*C*H), 76.12 (*C*H), 92.86 (*C*-1), 100.98 (*C*-1), 160.98 (C*q*), 169.09 (O*Ac*), 169.29 (O*Ac*), 169.46 (O*Ac*), 170.06 (O*Ac*), 170.17 (O*Ac*), 170.28 (O*Ac*), 170.50 (O*Ac*).

3.2.4. Methyl 1-*O*-(2-Carboxymethyl)-2,2',3,3',4',6,6'-hepta-*O*-acetyl-β-D-cellobiose (6)

α-D-Glucopyranose-4-*O*-(2,3,4,6-tetra-*O*-acetyl-β-D-glucopyranosyl)-2,3,6-triacetyl-1-*O*-trichloroacetimidate **5** (2.0 g, 2.56 mmol) and methyl glycolate (0.22 mL, 2.82 mmol) was stirred in dry CH_2Cl_2 (60 mL) over 4Å mol sieves at −25 ^{o}C. $BF_3.Et_2O$ (0.35 mL, 2.82 mmol) was added and the solution was allowed to warm slowly to room temperature. After 4-5 h, the solution was filtered and washed with sat. aq. $NaHCO_3$ soln. (2 × 20 mL), H_2O (2 × 20 mL) and brine (20 mL). The solvent was removed *in vacuo* the resulting residue was purified with column chromatography using EtOAc: hexane to yield a white solid (1.21 g, 67 %). IR (KBr); ν 2958 (C-H), 1756 (C=O), 1371 (CH), 1235 (O-C=O) and 1045 cm^{-1} (O-C-O); ^{1}H NMR ($CDCl_3$): δ 1.98 (3H, s, OAc), 2.01 (3H, s, OAc), 2.03 (6H, s, 2 × OAc), 2.08 (3H, s, OAc), 2.09 (3H, s, OAc), 2.12 (3H, s, OAc), 3.59 (1H, ddd, ^{3}J = 6.0, 3.0, 1.5 Hz, H-5'), 3.65 (1H, ddd, ^{3}J = 6.0, 3.0, 1.5 Hz, H-5), 3.74 (3H, s, OCH_3), 3.80 (1H, t, ^{3}J = 9.0 Hz), 4.00-4.10 (2H, m), 4.25 (2H, s, OCH_2CO_2Me), 4.36 (1H, dd, ^{3}J = 9.0, 3.0 Hz), 4.50-4.54 (2H, m), 4.69 (1H, d, ^{3}J = 7.8 Hz, H-1), 4.93-4.89 (2H, m), 5.06 (1H, t, ^{3}J = 9.1 Hz), 5.14

(1H, t, ^{3}J = 9.0 Hz), 5.21 (1H, t, ^{3}J = 9.0 Hz); ^{13}C NMR ($CDCl_3$): δ 20.55 (4 × CH_3), 20.67 (CH_3), 20.73 (CH_3), 20.85 (CH_3), 51.98 (OCH_3), 61.54 (*C-6*), 61.64 (*C*-6'), 65.10 (CH_2CO_2Me), 67.77 (*C*H), 71.19 (*C*H), 71.60 (*C*H), 71.93 (*C*H), 72.12 (*C*H), 72.83 (*C*H), 72.92 (*C*H), 76.29 (*C*H), 100.00 (*C*-1), 100.74 (*C*-1'), 169.01, 169.30, 169.51, 169.71, 169.86 , 170.23, 170.28, 170.50 (7 × OAc, 1 × CO_2Me).

3.2.5. 1-*O*-(2-Carboxamido)methyl-4-*O*-(β-D-glucopyranosyl)-β-D-glucopyranose (7)

Methyl 1-*O*-(2-carboxymethyl) 2,2',3,3',4,6,6'-hepta-*O*-acetyl-β-D-cellobiose **6** (1.5 g, 2.12 mmol) was stirred in a 2M NH_3 in MeOH soln. (30 mL, 60 mmol) for 1 h. The methanolic ammonia was removed under reduced pressure and the crude residue was recrystallised from a minimum of hot MeOH to yield a white solid (0.81 g, 97%). Mp 135.5 ^{o}C; IR (KBr): ν 3414 (OH and NH_2), 2917 (CH), 1675 (CO) and 1077 cm^{-1} (C-O-C); ^{1}H NMR (D_2O): δ 3.32 (1H, t, *J* = 9.0 Hz), 3.38-3.54 (4H, m), 3.58-3.68 (3H, m), 3.74 (1H, dd, ^{3}J = 12.3, 5.7 Hz), 3.83 (1H, dd, ^{3}J = 12.3, 4.8 Hz), 3.92 (1H, dd, ^{3}J = 12.3, 1.8 Hz), 3.98 (1H, dd, ^{3}J = 12.0, 1.8 Hz), 4.27 (1H, d, ^{3}J = 15.9 Hz, OCH_2CO_2Me), 4.39 (1H, d, ^{3}J = 15.9 Hz, OCH_2CO_2Me), 4.52 (1H, d, ^{3}J = 7.8 Hz, H-1), 4.55 (1H, d, ^{3}J = 7.8 Hz, H-1'); ^{13}C NMR (D_2O): δ 59.86 (CH_2), 60.58 (CH_2), 67.77 (OCH_2), 69.46 (*C*H), 72.73 (*C*H), 73.15 (*C*H), 74.11 (*C*H), 74.87 (*C*H), 75.50 (*C*H), 75.99 (*C*H), 78.43 (*C*H), 102.24 (C-1), 102.57 (C-1), 175.04 ($CONH_2$); calcd. $C_{14}H_{25}NO_{12}Na$, 422.1275; found 422.1249 [M+Na^{+}].

3.2.6. 1-*S*-(-2-Carboxamido)methyl-1-deoxy-1-thio-2,3,4,6-tetra-*O*-acetyl-β-D-glucopyranose (9)

To a solution of β-D-glucose pentaacetate **8** (9.8 g, 25.12 mmol) in MeCN was added $BF_3.Et_2O$ (3.08 mL, 37.5 mmol) followed by thiourea (1.91 g, 50.24 mmol). The solution was heated to reflux for 4 h. On cooling to room temperature, 2-chloroacetamide (2.34 g, 27.5 mmol) was added followed by Et_3N (10 mL). The solution was stirred for 1 h and the solvent removed *in vacuo*, the resulting syrup was dissolved in $CHCl_3$ (150 mL) and washed with H_2O (2 × 50 mL), brine (1 × 50 mL), dried ($MgSO_4$) and the solvent removed under reduced pressure. The resulting foam was recrystallised from hot MeOH to yield a pale yellow solid (5.1 g, 48 %). Mp 160.47 ^oC; IR (KBr) ν 3387 (NH), 2943 (CH), 1734 (C=O), 1644 (NHC=O), 1379 (CH), 1232 (O-C=O), 1031 (O-C-O) and 916 cm^{-1}; ^1H NMR ($CDCl_3$) δ 1.95 (3H, s, OAc), 1.97 (3H, s, OAc), 2.00 (3H, s, OAc), 2.03 (3H, s, OAc), 3.16 (1H, d, ^2J = 15.0 Hz, SCH_2CONH_2), 3.40 (1H, d, ^2J = 15.0 Hz, SCH_2CONH_2), 3.69 (1H, dt, ^3J = 9.3, 3.9 Hz, H-5), 4.12 (2H, d, ^3J = 3.9 Hz, H-6+6'), 4.53 (1H, d, ^3J = 9.3 Hz, H-1), 4.98 (1H, t, ^3J = 9.3 Hz, H-2), 5.01 (1H, t, ^3J = 9.3 Hz, H-4), 5.17 (1H, t, ^3J = 9.3 Hz, H-3), 5.75 (1H, br s, NH), 6.60 (1H, br s, NH'); ^{13}C NMR ($CDCl_3$): δ 20.15 (CH_3), 20.54 (CH_3), 20.62 (CH_3), 20.70 (CH_3), 33.78 (CH_2), 61.66 (*C*-6), 68.07 (*C*-4), 69.60 (*C*-2), 73.48 (*C*-3), 76.21 (*C*-5), 83.71 (*C*-1), 169.36 ($CONH_2$), 169.41 (O*Ac*), 170.04 (O*Ac*), 170.60 (O*Ac*), 171.26 (O*Ac*); Anal Calcd for $C_{16}H_{21}NO_{10}S$: C, 45.82; H, 5.05; N, 3.34. Found C, 45.45; H, 5.50, N, 3.21.

3.2.7 1-*S*-(-2-Carboxamido)methyl-1-deoxy-1-sulfinyl-2,3,4,6-tetra-*O*-acetyl-β-D-glucopyranose (10)

Oxone® (1.46 g, 4.77 mmol) was added to a solution of 1-*S*-(-2-carboxamido)methyl-1-deoxy-1-thio-2,3,4,6-tetra-*O*-acetyl-β-D-glucopyranose **9** (2.0 g, 4.77 mmol) in a 1:1 mixture of MeCN:H_2O (50 mL) and the mixture was stirred for 12 h. The solution was filtered and the solvent removed *in vacuo*. The syrup was dissolved in $CHCl_3$ (100 mL) and the organic

phase was washed with H_2O (2 × 20 mL), brine (20 mL), dried ($MgSO_4$) and the solvent removed under reduced pressure. The resulting foam was purified by column chromatography using EtOAc (100 %) as eluant to yield a white solid (0.15 g, 33 %) Mp 194.2 ^oC; IR (KBr) ν 3387 (NH), 2943 (CH), 1735 (C=O), 1644 (NHC=O), 1379 (CH), 1232 (O-C=O) and 1031 cm^{-1} (C-O-C); ^1H NMR ($CDCl_3$) δ 2.00 (3H, s, OAc), 2.06 (6H, s, 2 × OAc), 2.08 (3H, s, OAc), 3.64 (1H, d, ^2J = 15.0 Hz, S(O)CH_2CONH_2), 3.87 (1H, d, ^2J = 15.0 Hz, S(O)CH_2CONH_2), 4.11-4.26 (3H, m, H-6+6', H-5), 5.04 (1H, d, ^3J = 9.3 Hz, H-1), 5.05 (1H, t, ^3J = 9.3 Hz, H-4), 5.28 (1H, t, ^3J = 9.3 Hz, H-2), 5.47 (1H, t, ^3J = 9.3 Hz, H-3), 7.43 (1H, br s, NH), 7.81 (1H, br s, NH'). ^{13}C NMR δ_C: 20.28 (CH_3), 20.34 (CH_3), 20.49 (CH_3), 20.50 (CH_3), 54.62 (SCH_2CONH_2), 61.71 (*C*-6), 67.20 (*C*-2), 67.36 (*C*-4), 72.98 (*C*-3), 75.14 (*C*-5), 88.41 (*C*-1), 166.13 ($CONH_2$), 168.79 (O*Ac*), 169.2 (O*Ac*), 169.63 (O*Ac*), 170.01 (O*Ac*). $C_{16}H_{21}NO_{11}S$ calcd: C, 44.14; H, 4.86; N, 3.28; found C, 44.20; H, 4.83; N, 2.70. MS-ESI: Found m/z, 460.0857; calcd for $C_{16}H_{23}NO_{11}SNa$ [M+Na^+], 460.0890.

3.2.8 1-*S*-(-2-Carboxamido)-1-deoxy-1-sulfonyl-2,3,4,6-tetra-*O*-acetyl-β-D-glucopyranose (11)

Methyl 1-*S*-(-2-carboxamido)-1-deoxy-1-thio-2,3,4,6-tetra-*O*-acetyl-β-D-glucopyranose **9** (2.0 g, 4.77 mmol) was dissolved in $CHCl_3$ (60 mL) along with *m*CPBA (1.64 g, 9.54 mmol), the mixture was stirred for 30 min. The solution was filtered, and diluted with $CHCl_3$ (50 mL). The organic phase was washed with sat. $NaHCO_3$ soln. (2 x 20 mL), H_2O (2 x 20 mL), dried ($MgSO_4$) and the solvent removed under reduced pressure. The resulting foam was purified by column chromatography using EtOAc:hexane (90:10) as eluant to yield a white solid (1.35 g, 63 %) Mp 177.6 ^oC; IR (KBr) ν 3422 (NH), 2923 (CH), 1743 (C=O), 1672 (NHC=O), 1379 (CH), 1325 (O-C=O), 1222 (C-O-C), 1325 (SO_2) and 1132 cm^{-1} (SO_2); ^1H

NMR (d-DMSO): δ 1.95 (3H, s, OAc), 1.96 (3H, s, OAc), 2.00 (3H, s, OAc), 2.02 (3H, s, OAc), 3.97 (1H, d, ^{2}J = 15.0 Hz, $SO_2CH_2CONH_2$), 4.20 (1H, d, ^{2}J = 15.0 Hz, $SO_2CH_2CONH_2$), 3.98-4.08 (2H, m, H-6), 4.21-4.30 (1H, m, H-5), 4.96 (1H, t, ^{3}J = 4.8 Hz, H-4), 5.23 (1H, d, ^{3}J = 9.0 Hz, H-1), 5.39 (1H, t, ^{3}J = 9.0 Hz, H-2), 5.48 (1H, t, ^{3}J = 9.0 Hz, H-3), 7.49 (1H, br s, NH), 7.68 (1H, br s, NH'); ^{13}C NMR δ 20.18 (*C*H_3), 20.24 (*C*H_3), 20.33 (*C*H_3), 20.47 (*C*H_3), 55.10 (SO_2*C*H_2CONH_2), 61.34 (*C*-6), 65.68 (*C*-4), 67.21 (*C*-2), 72.70 (*C*-3), 74.88 (*C*-5), 85.75 (*C*-1), 162.37 (*C*ONH_2), 168.53 (O*Ac*), 169.20 (O*Ac*), 169.47 (O*Ac*), 170.03 (O*Ac*). MS-ESI: Found m/z, 476.0832; calcd for $C_{16}H_{23}NO_{12}SNa$ [$M+Na^+$], 476.0839.

3.3. Solid state characterisation

Single-crystal X-ray diffraction measurements for **7** were collected on a Bruker APEX II DUO diffractometer and a Bruker SMART X2S was used for **3** and **9**, as previously described.[21] A Rigaku FR-E+ diffractometer fitted with VariMax HF optics to give monochromatized Mo Kα radiation was used for **10** following previously described procedures.[22] Crystals suitable for analysis were obtained by recrystallisation from ethanol or methanol by slow evaporation. Calculations for **3**, **7** and **9** were made using the APEX2 v2009.3-0 software[23] incorporating the SHELX suite of programs for structure solution and refinement.[24] Calculations for **10** were made using CrystalClear-SM Expert 2.0 r13 software.[25] The structure was solved by Superflip[26] and refined using SHELXL-97.[24] All

diagrams were prepared using Mercury.[27] The small crystal size of **7** and the relatively large number of unobserved data (47%) contribute to the high R_{int} value.

Supplementary data

The crystallographic data on compounds **3**, **7**, **9** and **10** have been deposited with the Cambridge Crystallographic Data Centre, CCDC numbers 919648 - 919651**.** These data can be obtained free of charge from The Cambridge Crystallographic Data Centre via www.ccdc.cam.ac.uk/data_request/cif

Acknowledgments

This publication has emanated from research conducted with the financial support of Science Foundation Ireland under Grant Numbers 07/SRC/B1158 and 05/PICA/B802/EC07.

References

1. Braga, D.; Grepioni, F.; Maini, L. *Chem. Commun.* **2012**, *46*, 6232-6242; Braga, D.; Brammer, L.; Champness, N. R. *CrystEngComm*. **2005**, *7*, 1-19; Braga, D.; Grepioni, F. *Chem. Commun.* **2005**, *41*, 3635-3645; Braga, D. *Chem. Commun.* **2003**, *39*, 2751-2754; Desiraju, G. R. Curr. *Op. Solid State Mat. Sci.* **1997**, *2*, 451-454.

2. Ardizzone, S.; Dioguard, F. S.; Mussini, T.; Mussini, P. R.; Rondini, S.; Vercelli, B.; Vertova, A. *Cellulose* **1999**, *6*, 57-69; Garnier, S.; Petit, S.; Coquerel, G. *J. Thermal Anal. Calorimetry* **2002**, *68*, 489-502.

3. Desiraju, G. R.; *Angew. Chem. Int. Ed. Engl.* **1995**, *34*, 2311-2327.

4. Aakeröy, C. B.; Panikkattu, S. V.; DeHaven, B.; Desper, J. *Cryst. Growth Des.* **2012**, *12*, 2597-2587; Williams, L. J.; Jagadish, B.; Lansdown, M. G.; Carducci, M. D.; Mash, E. A. *Tetrahedron* **1999**, *55*, 14301-14322.

5. Seo, M.; Park, J.; Kim, S. Y. *Org. Biomol. Chem.* **2012**, *10*, 5332-5342; Kuduva, S. S.; Bläser, Boese, R.; Desiraju, G. R. *J. Org. Chem.* **2001**, *66*, 1621-1626.

6. Etter, M. C.; *Acc. Chem. Res.* **1990**, *23*, 120-126.

7. Cremer, D.; Pople, J. A. *J. Am. Chem. Soc.* **1975**, *97*, 1354-1358.

8. Pangborn, W.; Lange, D.; Pérez, S. *Int. J. Bio. Macromol.* **1985**, *7*, 363-369.

9. Kamitori, S.; Ueda, A.; Tahara, Y.; Yosida, H.; Ishii, T.; Uenishi, *J. Carbohyd. Res.* **2011**, *346*, 1182-1185.

10. Brooks, C. L.; Wimmer, K.; Kosma, P.; Müller-Loennies, S.; Brade, L.; Brade, H.; Evans, S. V. *Acta Cryst. F* **2013**, *F69*, 2-5.

11. Artner, D.; Stanetty, C.; Mereiter, K.; Zamyatina, A.; Kosma, P. *Carbohyd. Res.* **2011**, *346*, 1736-1746.

12. Mukherjee, A.; Jayaraman, N. *Tetrahedron* **2012**, *68*, 8746-8752.

13. Spek, A. L. *PLATON*; University of Utrecht: Utrecht, The Netherlands, 2000.

14. Yoneda, Y.; Mereiter, K.; Jaeger, C.; Brecker, L.; Kosma, P.; Rosenau, T.; French, A. *J. Am. Chem. Soc.* **2008**, *130*, 16678-16690.

15. Ham, J. T.; Williams, D. G. *Acta Cryst.* **1970**, *B26*, 1373-1383.

16. French, A. *Adv. Carbohyd. Chem. Biochem*. **2012**, *67*, 19-93.

17. French A. D.; Johnson, G. P. *Cellulose*, **2004**, *11*, 5-22.

18. Berkovitch-Yellin, Z.; Leiserowitz, L.; *J. Am. Chem. Soc.* **1980**, *102*, 7677-7681.

19. Schmidt, R. R.; *Angew. Chem. Int. Ed. Engl.* **1986**, *25*, 212-235.

20. Cai, B. T.; Lu, D.; Tang, X.; Zhang, Y.; Landerholm, M.; Wang, P. G.; *J. Org. Chem.* **2005**, *70*, 3518-3524.

21. Eccles, K. S.; Stokes, S. P.; Daly, C. A.; Barry, N. M.; McSweeney, S. P.; O'Neill, D. J.; Kelly, D. M.; Jennings, W. B.; Ni Dhubhghaill, O. M.; Moynihan, H. A.; Maguire, A. R.; Lawrence, S. E. *J. Appl. Cryst.*, **2011**, *44*, 213–215.

22. Coles, S. J.; Gale, P. A.; *Chem. Sci.*, **2012**, *3*, 683-689.

23. *APEX2 v2009.3-0; Bruker AXS: Madison, WI,* **2009**.

24. Sheldrick, G. M. *Acta Crystallogr. A,* **2008**, *64*, 112-122.

25. CrystalClear-SM Expert 2.0 r13 program suite, *Rigaku Corporation, Japan,* 2011.

26. Palatinus, L; Chapuis, G. *J. Appl. Crystallogr*., **2007**, *40*, 786-790.

27. Macrae, C. F.; Bruno, I. J.; Chisholm, J. A.; Edginton, P. R.; McCabe, P.; Pidcock, E.; Rodriguez-Monge, L.; Taylor R.; van de Streek, J.; Wood, P. A. *J. Appl. Crystallogr.* **2008**, *41***,** 466-470.

Figure Legends

Scheme 1. (a) $HOCH_2CO_2Me$, $BF_3.Et_2O$, CH_2Cl_2, −25 °C 4-5 h; (b) 2M NH_3 in MeOH, rt, 1 h; (c) $BnNH_2$, THF, rt, 12 h; (d) CCl_3CCN, DBU, CH_2Cl_2, 0 °C, 30 mins then rt, 12 h.

Figure 1. View of crystal structure of compound **3** showing discrete hydrogen bond between primary amide N-H and pyranose oxygen forming C(7) chains.

Figure 2. Illustration of discrete hydrogen bond between primary amide N-H and pyranose oxygen forming C(7) chains of compound **3** (depicted in red).

Figure 3. View of crystal structure of compound **3** showing C(17) chains resulting from amide N-H hydrogen bond donation (to pyranose oxygen) and amide oxygen hydrogen bond acceptance (from primary hydroxyl) in compound **3**.

Figure 4. Illustration of C(17) chains resulting from amide N-H hydrogen bond donation (to pyranose oxygen) and amide oxygen hydrogen bond acceptance (from primary hydroxyl) in compound **3** (depicted in red).

Figure 5. View of the crystal structure of **7**.MeOH solvate showing hydrogen bonding interactions of the primary amide groups.

Figure 6. Illustration of the hydrogen bonding interactions of the primary amide groups in the structure of **7**.MeOH solvate.

Figure 7. View of the crystal structure of **7**.MeOH solvate showing intramolecular S(7) and S(9), and intermolecular $R_3^3(9)$ hydrogen bonding motifs in the structure of **7**.MeOH solvate.

Figure 8. Intramolecular S(7) (depicted in blue), S(9) (depicted in green), and intermolecular $R_3^3(9)$ (depicted in red), hydrogen bonding motifs in the structure of **7**.MeOH solvate.

Figure 9. Cross layering of cellobioside moieties of **7**.MeOH viewed along the crystallographic *b* axis.

Scheme 2. (a) NH_2CSNH_2, $BF_3.Et_2O$, MeCN, Δ, 4 h, then $ClCH_2CONH_2$, Et_3N, rt, 1 h; (b) Oxone®, MeCN, H_2O, rt, 12 h; (c) mCPBA, $CHCl_3$, 0 °C, rt, 30 mins.

Figure 10. View of the crystal structure of compound **9** showing hydrogen bonding interactions of the primary amide group.

Figure 11. Illustration of hydrogen bonding interactions of the primary amide group in the structure of compound **9**.

Figure 12. View of the crystal structure of compound **10** showing hydrogen bonding interactions of the primary amide group.

Figure 13. Illustration of hydrogen bonding interactions of the primary amide group in the structure of compound **10** forming $R_3^2(8)$ hydrogen bond patterns (depicted in red).

Figure 14. Packing of molecules of compound **10.**

Table 1. Crystallographic data

Compound reference	**3**	**7**	**9**	**10**
Chemical formula	$C_8H_{15}NO_7$	$C_{15}H_{29}NO_{13}$	$C_{16}H_{23}NO_{10}S$	$C_{16}H_{23}NO_{11}S$
Formula mass	237.21	431.39	421.41	437.41
Crystal system	Monoclinic	Monoclinic	Orthorhombic	Monoclinic
a/Å	5.5981(8)	9.651(3)	7.3864(9)	9.1221(9)
b/Å	6.9551(9)	8.387(3)	13.496(2)	5.5092(5)
c/Å	13.5890(17)	12.638(5)	20.100(3)	21.085(2)
β/°	101.378(4)	105.322(13)	90	91.474 (6)
V/Å^3	518.69(12)	986.6(6)	2003.7(5)	1059.29(17)
Radiation used	Mo Kα	Mo Kα	Cu Kα	Cu Kα
Crystal size/mm	0.45 x 0.32 x 0.22	0.11 x 0.09 x 0.06	0.47 x 0.23 x 0.17	0.20 x 0.01 x 0.01
Temperature/K	300(2)	296(2)	300(2)	100(2)
Space group	$P2_1$	$P2_1$	$P2_12_12_1$	$P2_1$
Z	2	2	4	2
μ/mm^{-1}	0.134	0.128	0.215	0.209
No. of reflections measured	3715	10491	19356	5623
No. of independent reflections	2038	3813	3823	4311
R_{int}	0.0199	0.0908	0.0283	0.0352
Final R_1 values ($I > 2\sigma(I)$)	0.0345	0.0534	0.0297	0.0739
Final $wR(F^2)$ values ($I > 2\sigma(I)$)	0.0840	0.0758	0.0864	0.1131
Final R_1 values (all data)	0.0399	0.1380	0.0367	0.0532
Final $wR(F^2)$ values (all data)	0.0878	0.0976	0.1005	0.1131
Goodness of fit on F^2	1.055	0.950	1.123	1.044
Flack parameter	-1.8(11)	1.7(15)	-0.01(7)	-0.10(11)

Table 2. Hydrogen bond data

Donor-H···Acceptor	ARU	D-H	H···A	D···A	D-H···A
Compound 3					
N(11)-H(11A)···O(6)	*-x, 0.5+y, 1-z*	0.87(3)	2.18(3)	3.021(3)	162(3)
N(11)-H(11B)···O(7)	Intramolecular	0.87(3)	2.26(3)	2.648(3)	107(2)
O(12)-H(12)···O(16)	*-1+x, 1+y, z*	0.82	2.16	2.851(2)	142
O(13)-H(13)···O(14)	Intramolecular	0.82	2.56	2.8866(18)	105
O(13)-H(13)···O(12)	*-x, -0.5+y, 2-z*	0.82	2.08	2.8743(19)	162
O(14)-H(14)···O(13)	*-x, -0.5+y, 2-z*	0.82	1.86	2.6683(18)	168
O(16)-H(16)···O(10)	*1-x, -0.5+y, 1-z*	0.82	1.96	2.768(2)	171
C(3)-H(3)···O(14)	*1-x, 0.5+y, 2-z*	0.98	2.32	3.269(2)	163
C(5)-H(5)···O(13)	*1+x, y, z*	0.98	2.45	3.398(2)	164
C(8)-H(8A)···O(6)	Intramolecular	0.97	2.43	2.816(2)	104
C(8)-H(8A)···O(10)	*1-x, -0.5+y, 1-z*	0.97	2.51	3.456(3)	166
C(15)-H(15A)···O(14)	Intramolecular	0.97	2.59	2.984(2)	105
Compound 7					
N(9)-H(9A)···O(24)	*1-x, 1.5+y, 1-z*	0.86	2.26	3.079(4)	159
N(9)-H(9B)···O(7)	Intramolecular	0.86	2.27	2.653(4)	107
N(9)-H(9B)···O(12)	*1-x, 0.5+y, 1-z*	0.86	2.39	3.185(5)	153
O(11)-H(11)···O(12)	*1-x, 0.5+y, 1-z*	0.82	1.95	2.728(4)	157
O(12)-H(12)···O(13)	Intramolecular	0.82	2.56	2.944(4)	110
O(12)-H(12)···O(19)	Intramolecular	0.82	1.95	2.762(4)	169
O(20)-H(20)···O(22)	*2-x, 0.5+y, 2-z*	0.81(5)	2.05(5)	2.837(5)	167(5)
O(21)-H(21)···O(28)	*1-x, -0.5+y, 2-z*	0.82	1.91	2.724(5)	173
O(22)-H(22)···O(26)	*2-x, -0.5+y, 2-z*	0.82	1.93	2.748(4)	177
O(24)-H(24)···O(11)	*1-x, -0.5+y, 1-z*	0.82	2.08	2.882(4)	165
O(26)-H(26)···O(21)	*x, 1+y, z*	0.82	1.94	2.716(4)	158
O(28)-H(28)···O(10)	*x, -1+y, z*	0.82	1.87	2.599(6)	148
C(2)-H(2)···O(24)	*x, 1+y, z*	0.98	2.60	3.516(5)	156
C(5)-H(5)···O(20)	*1-x, 0.5+y, 2-z*	0.98	2.59	3.175(6)	118
Compound 9					
N(11)-H(11A)···O(6)	*-0.5+x, 2.5-y, -z*	0.86	2.24	3.045(2)	155
N(11)-H(11B)···O(14)	*-1+x, y, z*	0.86	2.15	2.978(3)	163
C(2)-H(2)···O(14)	Intramolecular	0.98	2.32	2.719(3)	104
C(2)-H(2)···O(10)	*0.5+x, 2.5-y, -z*	0.98	2.47	3.330(3)	146
C(3)-H(3)···O(18)	Intramolecular	0.98	2.35	2.725(3)	102
C(4)-H(4)···O(22)	Intramolecular	0.98	2.31	2.686(2)	102
C(15)-H(15B)···O(22)	*0.5-x, 2-y, -0.5+z*	0.96	2.46	3.289(3)	145
C(19)-H(19C)···O(12)	*0.5+x, 1.5-y, -z*	0.96	2.56	3.438(3)	152
C(23)-H(23A)···O(27)	*-x, -0.5+y, 0.5-z*	0.96	2.51	3.461(4)	171
C(24)-H(24B)···O(10)	*-0.5+x, 2.5-y, -z*	0.97	2.58	3.331(3)	134

C(28)-H(28B)···O(22)	*-1+x, y, z*	0.96	2.39	3.295(4)	157
Compound 10					
N(1)-H(1A)···O(3)	*1-x, 0.5+y, 1-z*	0.88	1.99	2.871(4)	175
N(1)-H(1B)···O(2)	*x, 1+y, z*	0.88	2.29	3.074(4)	149
C(2)-H(2)···O(11)	Intramolecular	1.00	2.25	2.646(4)	102
C(3)-H(3)···O(9)	Intramolecular	1.00	2.25	2.701(5)	106
C(4)-H(4)···O(7)	Intramolecular	1.00	2.30	2.725(4)	104
C(5)-H(5)···O(7)	*x, -1+y, z*	1.00	2.37	3.346(4)	165
C(6)-H(6B)···O(2)	*x, 1+y, z*	0.99	2.08	3.007(4)	156
C(10)-H(10A)···O(5)	*1-x, -0.5+y, -z*	0.98	2.56	3.501(5)	161
C(10)-H(10B)···O(5)	*x, -1+y, z*	0.98	2.60	3.406(5)	140
C(12)-H(12B)···O(5)	*-1+x, y, z*	0.98	2.50	3.440(5)	161
C(14)-H(14A)···O(2)	*-1+x, 1+y, z*	0.98	2.47	3.284(5)	140
C(14)-H(14B)···O(9)	*x, 1+y, z*	0.98	2.51	3.315(5)	139

Table 3. Cremer-Pople ring puckering coordinates[7]

Compound	Q / Å	θ / °	φ / °
3	0.573(18)	8.38(18)	34.3(13)
7 (reducing end)	0.574(4)	6.4(4)	73(4)
7 (non-reducing end)	0.605(2)	7.9(4)	354(3)
9	0.575(19)	3.42(18)	354(3)
10	0.563(3)	11.1(4)	76.4(18)

Scheme 1

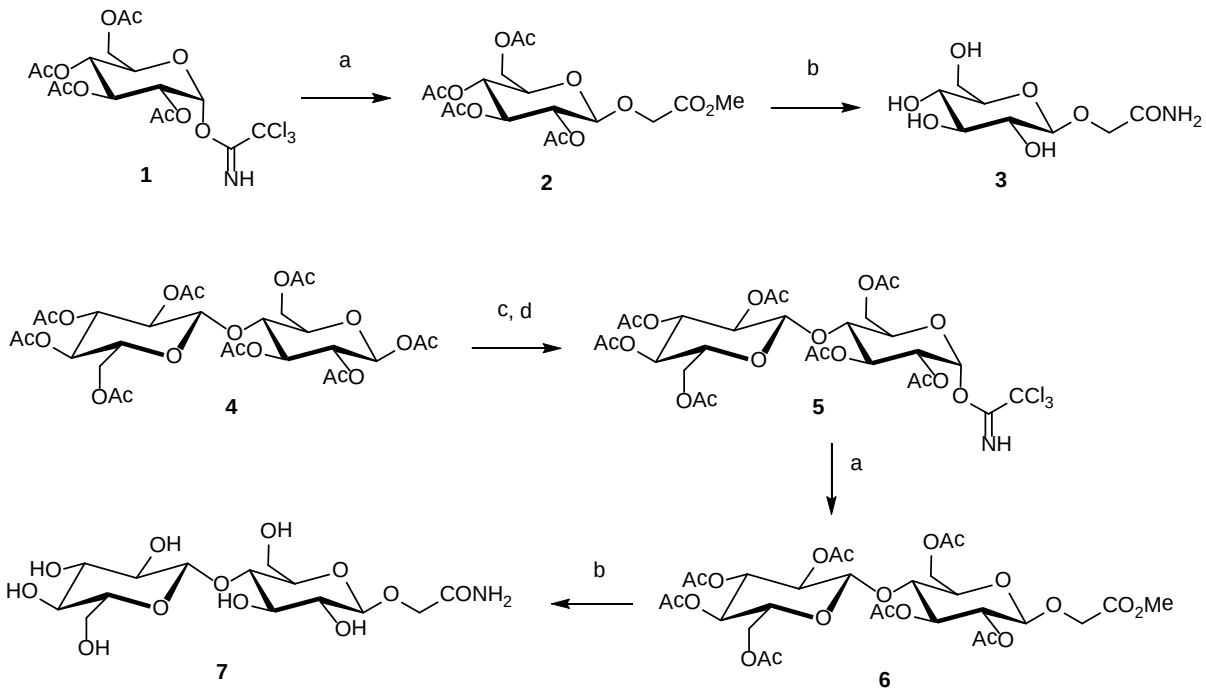
OAc
AcO
AcO
AcO
O
CCl3
NH
1
a
OAc
AcO
AcO
AcO
O
O
CO2Me
2
b
OH
HO
HO
O
O
CONH2
OH
3
OAc
AcO
AcO
O
OAc
4
c, d
OAc
AcO
AcO
O
OAc
5
a
OAc
AcO
AcO
O
OAc
6
b
OH
HO
HO
O
OH
7

Figure 1

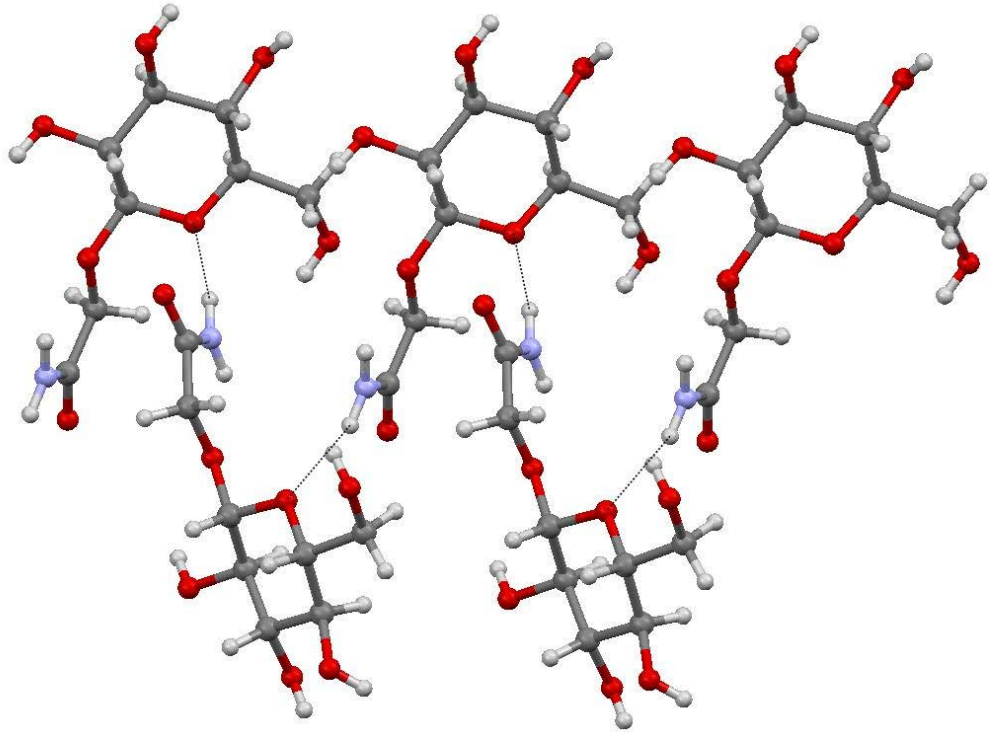

Figure 2

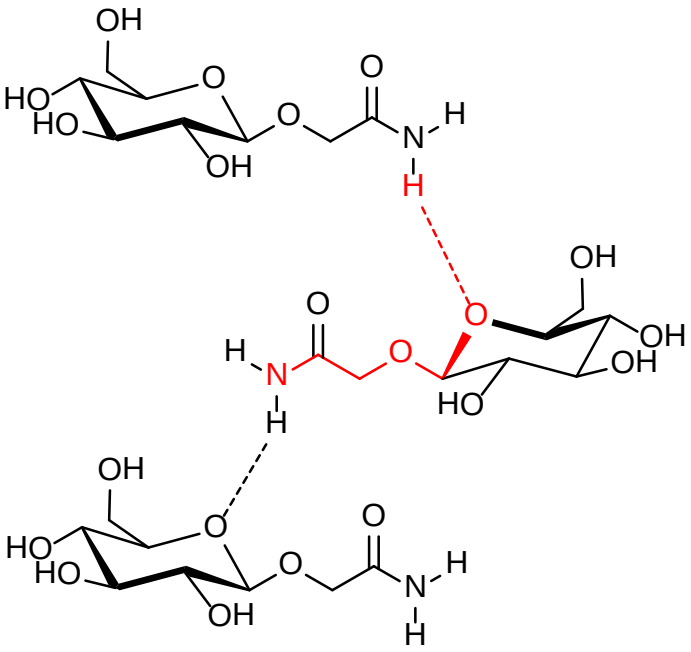

Figure 3

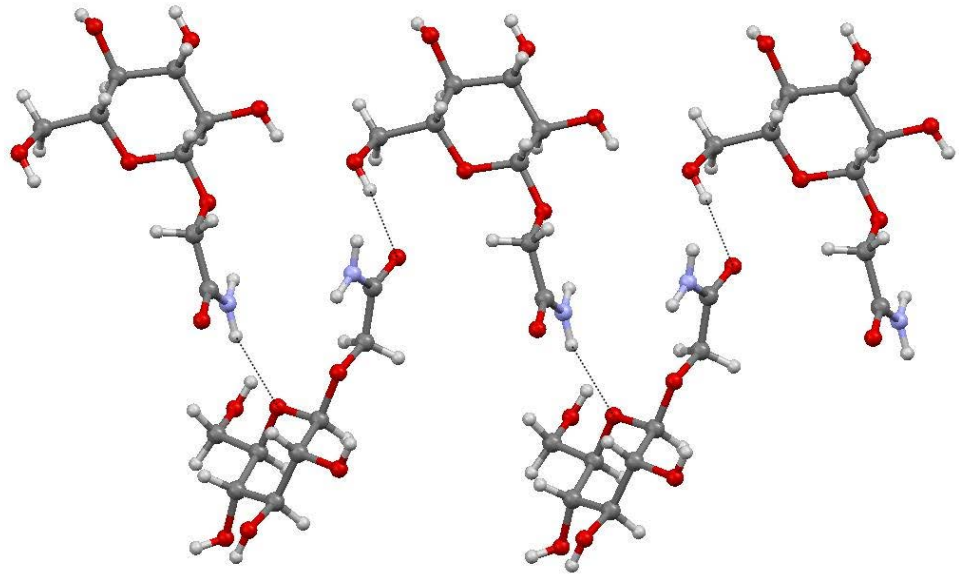

Figure 4

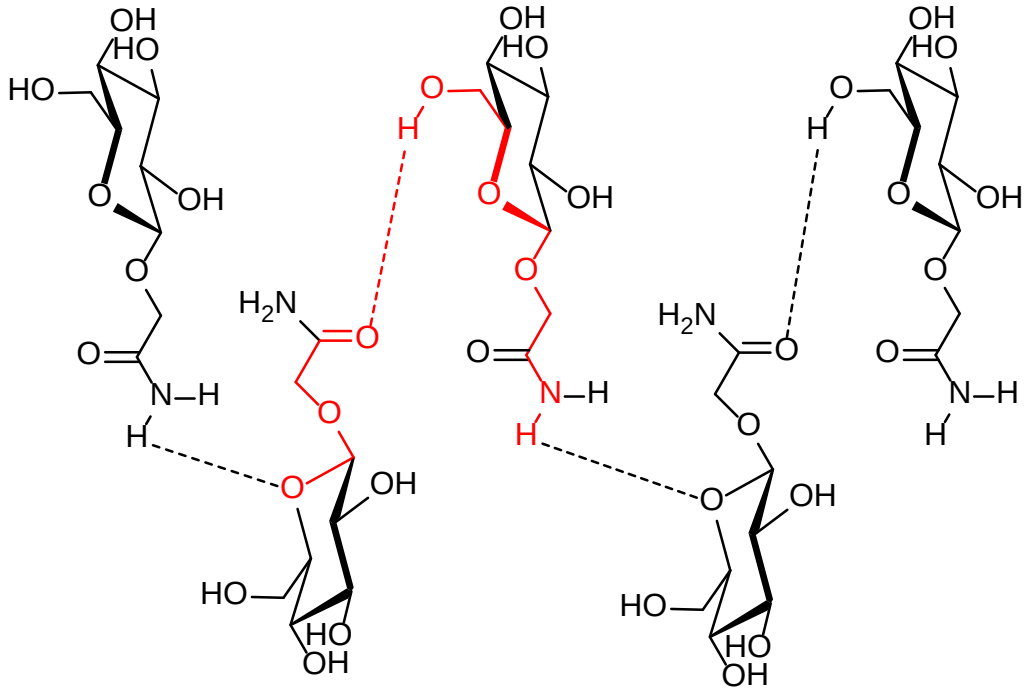
OH
HO
HO
O
OH
O
O
N–H
H
O
H
O
H2N
O
O
OH
HO
HO
OH
OH
HO
O
H
O
OH
O
O
N–H
H
O
H2N
O
O
OH
HO
HO
OH
OH
HO
O
H
O
OH
O
O
N–H
H

Figure 5

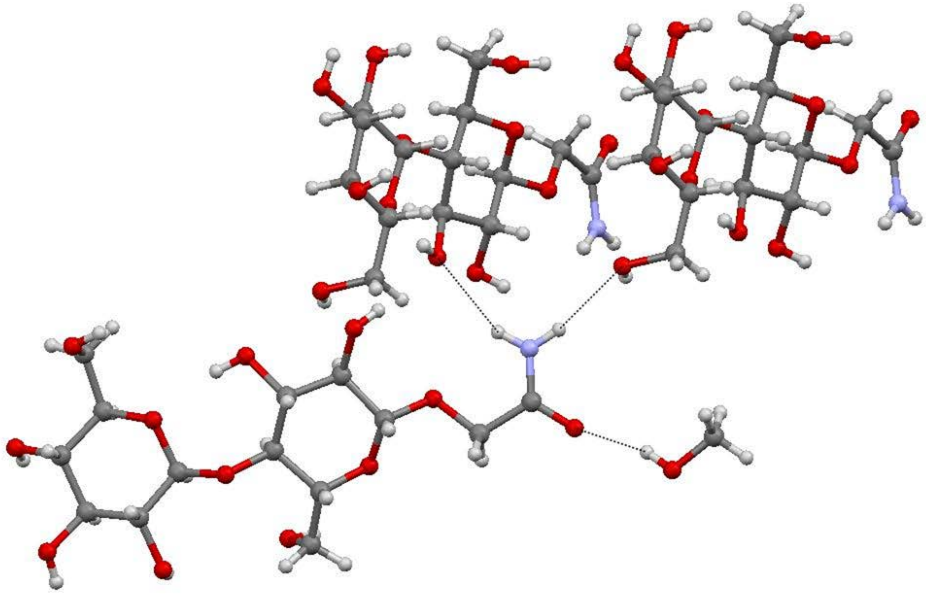

Figure 6

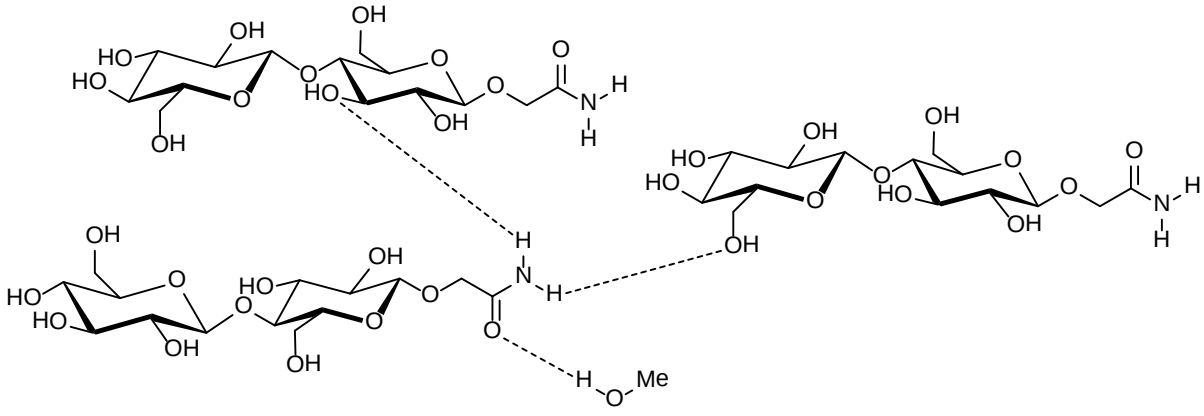

Figure 7

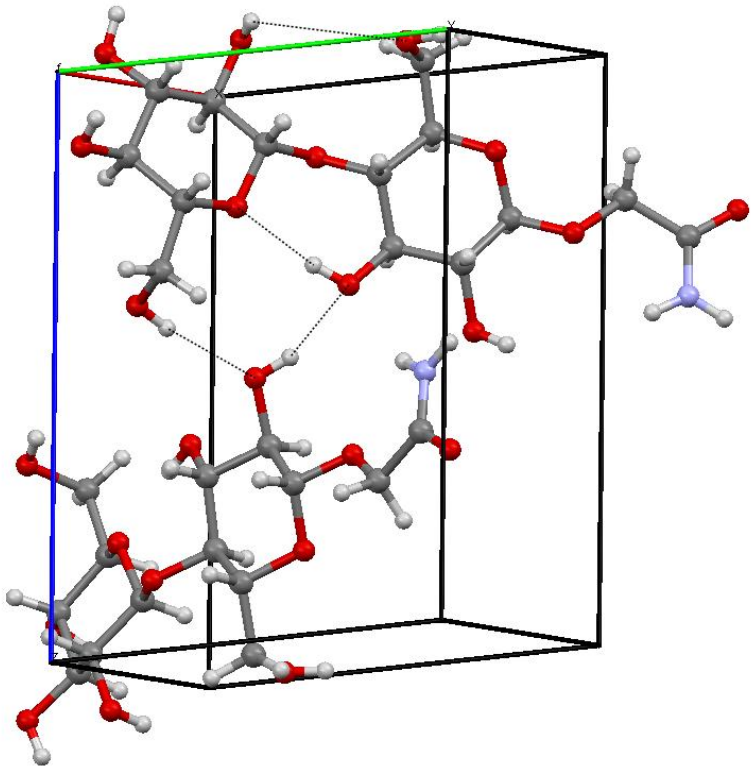

Figure 8

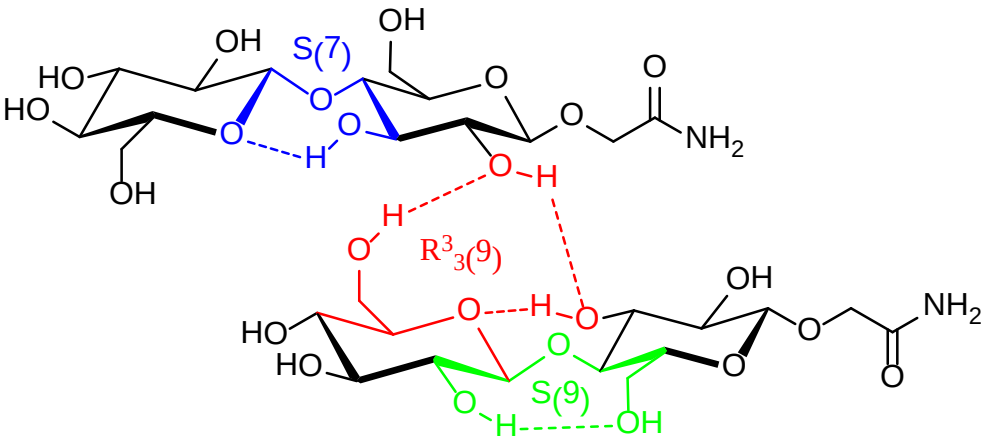
OH
S(7)
OH
HO
HO
O
O
O
O
O
NH2
H
OH
O
H
H
O
R33(9)
O
H
O
OH
NH2
HO
HO
O
O
O
S(9)
O
H
OH

Figure 9

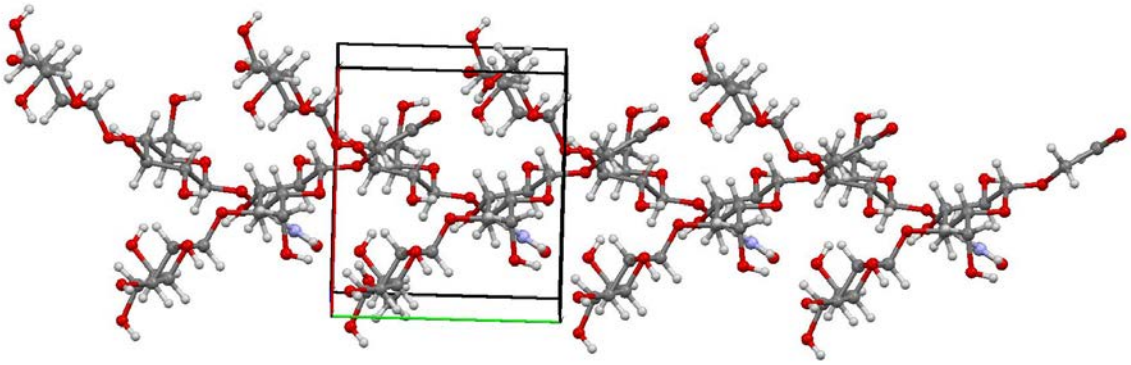

Scheme 2

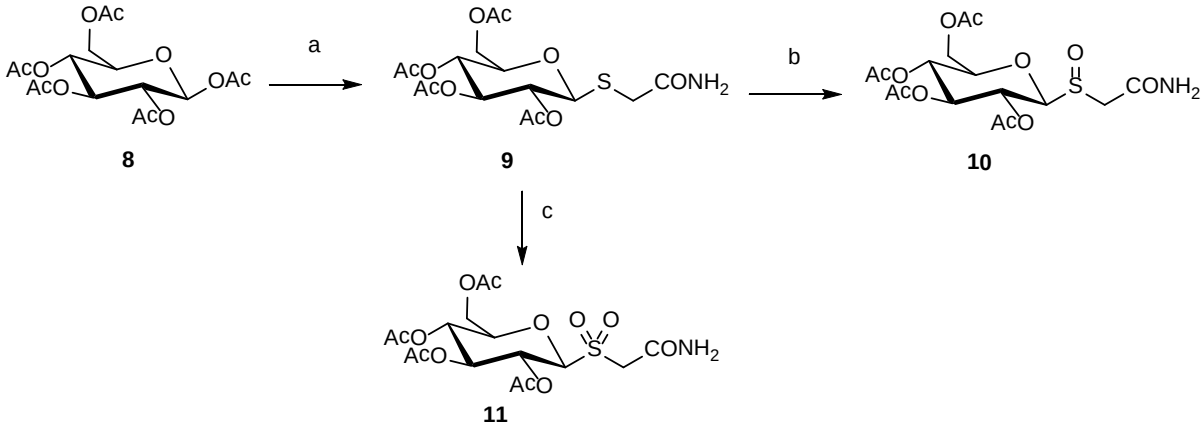

Figure 10

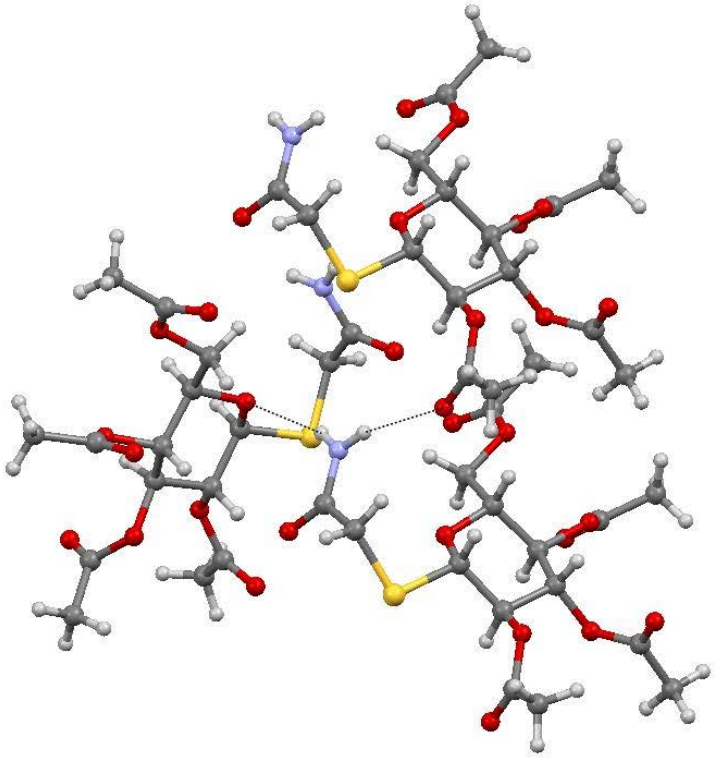

Figure 11

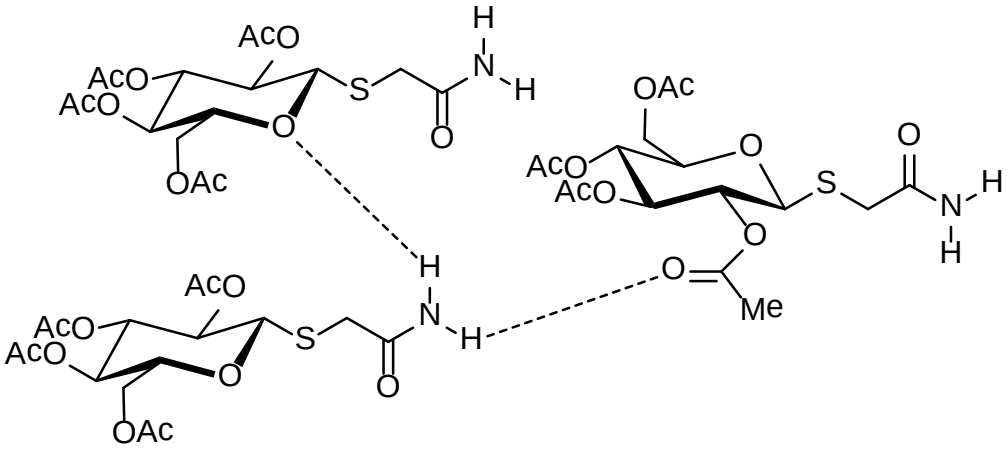
AcO
AcO
AcO
OAc
O
S
H
N
H
O
OAc
AcO
AcO
O
S
O
N
H
H
O
Me
H
N
H
AcO
AcO
AcO
OAc
O
S
O

Figure 12

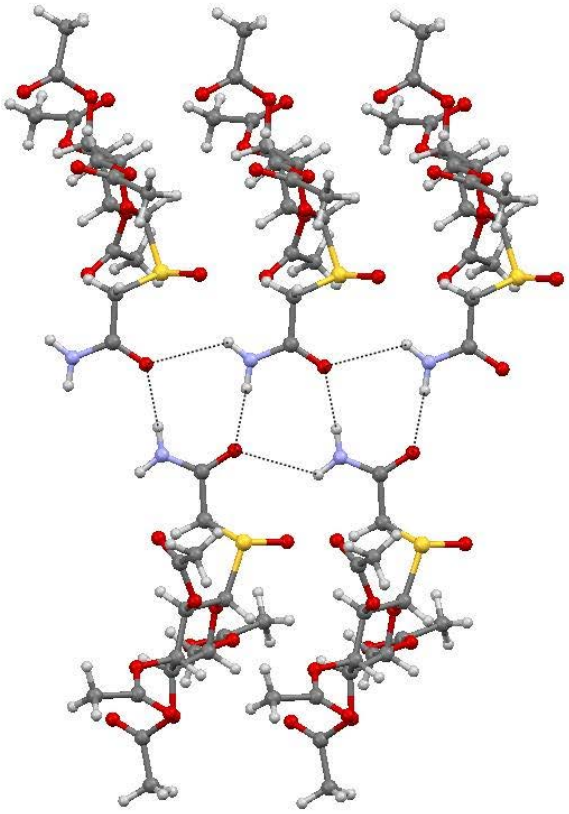

Figure 13

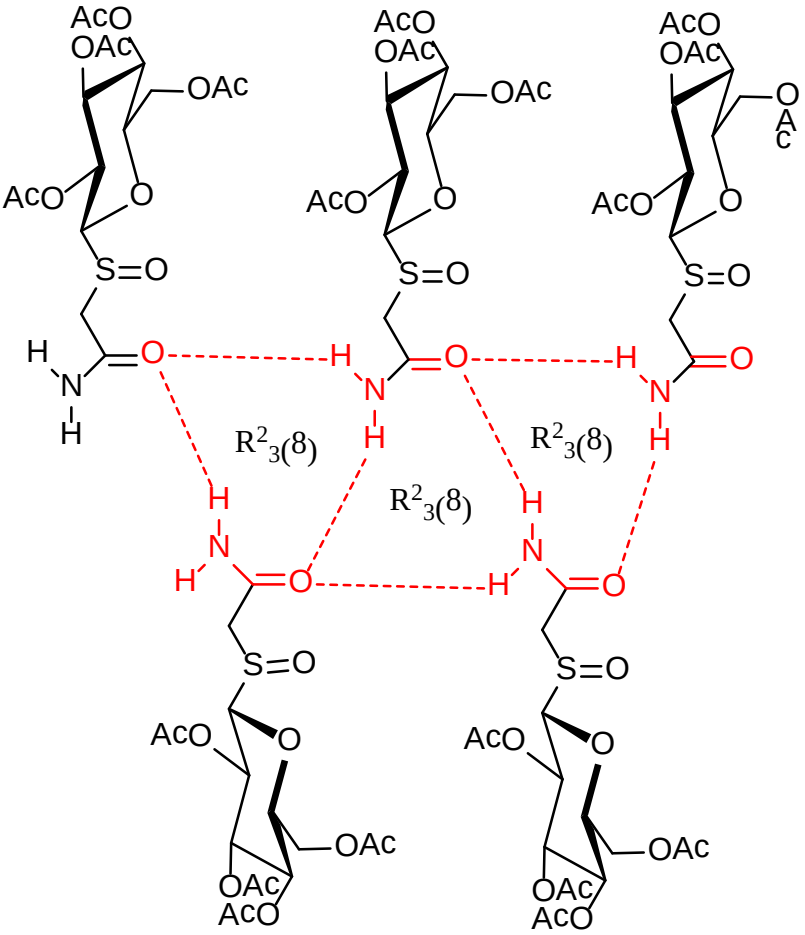
AcO
OAc
OAc
AcO
O
S=O
H
N
H
O
H
N
H
O
H
N
H
O
$R^2_3(8)$
$R^2_3(8)$
$R^2_3(8)$
H
N
H
O
H
N
H
O
S=O
AcO
O
OAc
OAc
AcO

Figure 14